PHYSICAL REVIEW B **86**, 045442 (2012)

Atomic structure and spectroscopy of graphene edges on Ir(111)

Soo-hyon Phark,[1,*] Jérôme Borme,[1,2] A. León Vanegas,[1] Marco Corbetta,[1] Dirk Sander,[1] and Jürgen Kirschner[1]
[1]*Max-Planck-Institut für Mikrostrukturphysik, Weinberg 2, 06120 Halle, Germany*
[2]*International Iberian Nanotechnology Laboratory, Avenida Mestre José Veiga, 4715-310 Braga, Portugal*

(Received 9 January 2012; revised manuscript received 11 May 2012; published 25 July 2012)

We performed scanning tunneling microscopy/spectroscopy (STM/S) on the edges of monolayer graphene islands grown on Ir(111). Constant current STM images reveal that the atomic corrugation at the graphene edges correlates with the moiré pattern of graphene on Ir(111). The graphene islands terminate with a zigzag edge and moiré-periodic kinks in the regions of the on-top stacked carbon rings. Graphene edges near an Ir(111) monatomic step also show the formation of periodic kinks. STS indicates a significant spatial dependence of the differential conductance dI/dV near graphene edges. We observe a considerably reduced differential conductance at the graphene island edges. We tentatively ascribe these observations to the electronic interaction of graphene with the Ir(111) substrate, which affects the differential conductance differently near graphene edges as compared to the inner part of a graphene island.

DOI: 10.1103/PhysRevB.86.045442 PACS number(s): 68.65.Pq, 68.37.Ef, 68.55.A−, 73.22.Pr

Graphene (G) has attracted significant attention because of its special and unique physical properties which make it a promising future material for nanoelectronics.[1] In nanosize G structures the increased edge-to-area ratio is expected to influence the electronic properties of G significantly. Edge-localized electrons in a free-standing G nanoribbon were proposed by Nakada *et al.*[2] Magnetic ordering and electronic spin polarization near the zigzag edge were predicted.[3]

Various efforts have been devoted to measure the electronic properties of G edges on SiO_2,[4] Ir(111),[5] graphite,[6] SiC,[7] and other substrates.[8] An atomically resolved measurement was realized very recently by Tao *et al.*[9] for G nanoribbons produced from unrolled single-wall carbon nanotubes. However, the experimental database on the correlation between atomic structures and electronic properties for the edges of G islands on metallic substrates is still scarce, and we report results on G edges on Ir(111).

A theoretical study[10] predicts a small binding energy of ≈50 meV per C atom in G/Ir(111). G π-band related features were observed in angle-resolved photoemission spectroscopy (ARPES) studies of G/Ir(111).[11,12] In addition, scanning tunneling microscopy (STM) studies[13–15] indicate a dominance of zigzag edge termination in G/Ir(111), which is promising for the study of the edge-localized electrons.[2,3] However, a strong edge-substrate interaction of G/Ir(111) has been proposed.[16] Thus, a spatially resolved investigation of spectroscopic features of G/Ir(111) is called for to elucidate the influence of the substrate on the electronic states near a G edge.

Here we present an STM and scanning tunneling spectroscopy (STS) study focusing on the edges of G islands on Ir(111) with atomic resolution. The atomic corrugation near a G edge shows a strong correlation with the stacking sites of the edge atoms, and it is correlated to the moiré pattern of G/Ir(111). Reduction of the differential conductance dI/dV at G edges reflects a change of the G electronic structures which we ascribe to the different G-Ir interaction near the edges as compared to the central region of the G island.

The experiments were performed in an ultrahigh vacuum chamber (base pressure $< 2\times10^{-11}$ mbar) equipped with a scanning tunneling microscope operating at 8 K. The Ir(111) single crystal (MaTeck GmbH) was cleaned by the repetition of Ar^+ sputtering (1 keV, 0.75 μA, 15 min per cycle) and subsequent heating in an O_2 pressure of 1×10^{-8} mbar up to 1200 K. In order to grow monolayer G, the cleaned substrate was exposed to C_2H_4 at 300 K at a pressure of 2×10^{-9} mbar for 2 min and subsequently heated to the flash temperature $T_{\text{flash}} = 1320$ K. Overall heating process took 2 min and then the heater was switched off as soon as the substrate temperature reached T_{flash}. The pressure of the chamber increased up to 1×10^{-8} mbar at T_{flash}. Constant-current STM (CC-STM) images show that ~40% of the substrate surface was covered by G islands. The island size ranged from 6 to 50 nm in diameter and only single layer islands were observed.[17] We employed a lock-in technique with a modulation bias voltage V_b at a frequency $\nu = 4$ kHz and root-mean square amplitude of 20 mV to detect $I(V)$ and dI/dV simultaneously.

Figure 1(a) shows edges of a G island on Ir(111). The CC-STM image measured on the central part of the G island shows a clear honeycomb structure as shown in the inset of Fig. 1(a). It also reveals a pattern with a periodicity of 2.52 ± 0.03 nm, regardless of the size and shape of the islands, as indicated by the gray mesh. This pattern is known as moiré structure, and it is attributed to the periodic change in the electronic interaction between G and the Ir(111) substrate.[10] The moiré pattern identifies the formation of an epitaxially ordered G monolayer. Different stacking sites of the C ring center allow us to distinguish three regions within the moiré unit cell.[13] We label these regions as "ONT," "FCC," and "HCP" regions, where the center of the C rings stack on the on-top, fcc, and hcp sites of the Ir(111) lattice, respectively. We identify the bright circular CC-STM contrast in the G island as an ONT region due to its circular symmetry.[13] In Fig. 1 the crossing points of the gray mesh are located at the centers of the ONT regions.

We observe two typical types of G/Ir(111) edges. Figures 1(b) and 1(c) are sketches of the cross sections along the yellow and blue dashed arrows in Fig. 1(a), respectively. We distinguish between *steplike* and *borderlike* edges. They represent G edges on an Ir(111) surface and at an Ir(111) step

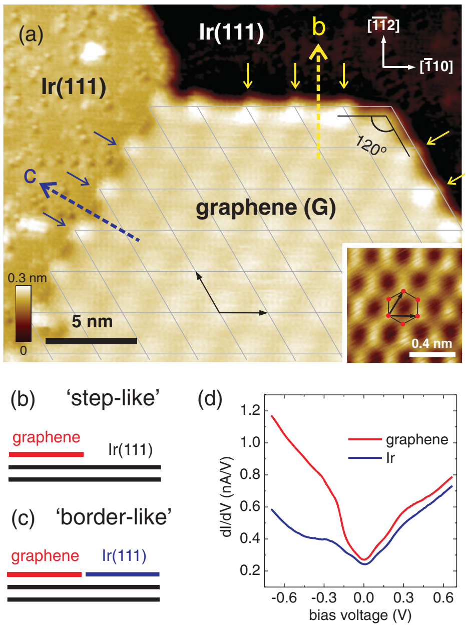

FIG. 1. (Color online) (a) CC-STM image of edges of graphene (G) on Ir(111) ($V_b = -0.3$ V, $I_{\text{set}} = 1$ nA). Crystallographic directions of the Ir substrate are denoted at the top-right side. The gray mesh indicates the moiré superstructure on G. The crossing points are located at the centers of ONT regions.[13] The moiré lattice vectors are drawn as black arrows. (b) and (c) are the side-view illustrations of the surface layers along the dashed yellow and blue arrows. They represent edges on an Ir(111) surface and at an Ir(111) step edge, called *steplike* and *borderlike* edges, respectively. The inset is an STM image of the G lattice with an illustration of the hexagonal C ring (red spheres) and lattice vectors (black arrows) ($V_b = 0.05$ V, $I_{\text{set}} = 1$ nA). (d) STS spectra measured on the central region of G and on the Ir(111) terrace.

edge, respectively. Note that both edges are parallel to the moiré high symmetry directions. The edges are corrugated with the same periodicity as the moiré structure and they protrude at the ONT regions, as indicated by yellow and blue arrows in Fig. 1(a).[14] Thus the periodic protrusion of the ONT stacking region at the edges suggests a strong influence of the C stacking configuration on the edge formation of G on Ir(111).

Figure 1(d) shows STS spectra measured on the central region of G and on the Ir(111) substrate. The curves represent the spatial average of ∼200 spectra, taken over the area of one G moiré cell to average out the moiré-induced change of the dI/dV signal. The shapes of the dI/dV spectra taken at G and Ir are similar. The dI/dV spectra reveal that the difference between spectra taken at G and Ir is much more pronounced in the negative V_b regime as compared to the positive regime. Recent works[10,18] suggest a considerable electronic interaction between G and Ir. It remains a topic of future works to elucidate the role of an electronic interaction between Ir and G for the specific shape and amplitude of the dI/dV signals.

To examine the edge structures in detail, we measure atomically resolved CC-STM images. Figure 2(a) shows a *steplike* edge of G/Ir(111). The edge is almost parallel to a $\langle\bar{1}10\rangle$ direction of Ir. It shows periodic kinks protruding towards the Ir region, as indicated by the black arrows. The measured distance between two neighboring kinks is ≈2.5 nm, which corresponds to the moiré periodicity. CC-STM image for a smaller region, indicated by the white box in Fig. 2(a), allows us to see clearly the atomic lattices of both Ir(111) and G as shown in the image of Fig. 2(b). The white mesh is the registry of the substrate Ir atoms, as obtained from the atomically resolved Ir(111) surface. We extend it over the whole area of the image to identify the on-top-stacked C rings in the G area. Thus we obtain Fig. 2(e) as the model of the atomic configurations for the G edges shown in Fig. 2(b). The kinks at the ONT regions are connected by the straight ridges of a zigzag edge.[15] In Fig. 1(a) one can see two *steplike* edges which enclose an angle of 120°. An ONT region is composed of C atoms located at the hollow (fcc or hcp) sites of Ir(111).[13] If the outermost atoms of the kink of one edge are located on the fcc sites, those of the other should be on the hcp sites. Note that the protruding kinks occur at the ONT regions in both cases. This implies that both types of hollow sites are favorable for the edge atoms of *steplike* edges. Further work may identify the relative significance of strain and electronic structure related to energy contributions to the formation of the specific edge morphology. This would lead to an improved understanding of the driving

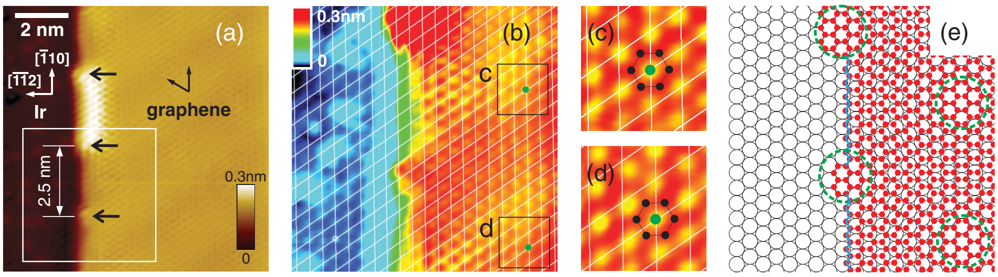

FIG. 2. (Color online) (a) CC-STM image of a *steplike* G edge ($V_b = -0.1$ V, $I_{\text{set}} = 1$ nA). Black arrows indicate periodic kinks along the edge. (b) CC-STM image of the boxed region in (a) with atomic resolution on both Ir (left side, blue) and G (right side, yellow-red) ($V_b = -0.1$ V, $I_{\text{set}} = 1$ nA). (c) and (d) are the 1×1 nm^2 zooms of the squared regions in (b). Cross points of meshes and green dots correspond to the on-top sites of the Ir lattice and on-top-stacked C rings, respectively, in (b), (c), and (d). Honeycomb C rings are overlaid in (c) and (d) in order to clarify the C atomic positions. (e) Model illustrating the superposition of the Ir and G lattices. The C stacking configurations are chosen for ONT regions to match those identified in (b). Red spheres and black circles represent C and Ir atoms, respectively. Green dashed circles in (b) and (e) denote the ONT regions. Cyan folded lines denote the zigzag arrangement of edge C atoms.

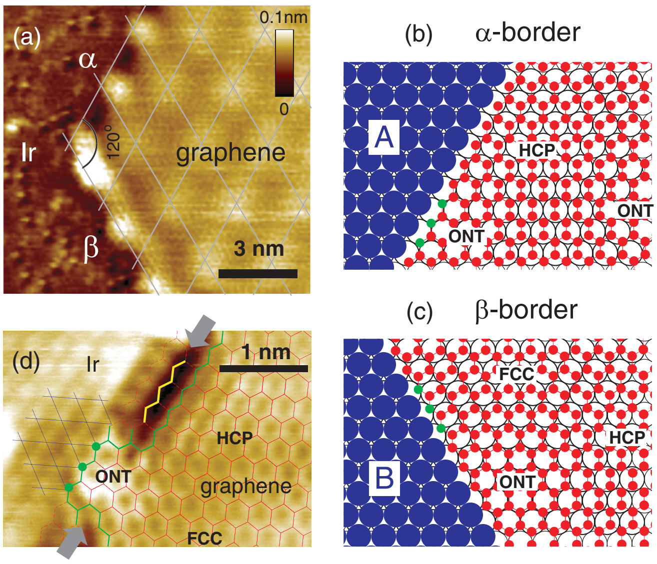

FIG. 3. (Color online) (a) CC-STM image of *borderlike* G edges ($V_b = -0.3$ V, $I_{\rm set} = 1$ nA). The mesh indicates the moiré lattice with ONT regions located at the crossing points. (b) and (c) show hard sphere models of the atomic stacking positions of G sheet near A and B steps of Ir(111), respectively. Red spheres, blue spheres, and black circles represent the G carbon, surface Ir, and underlying Ir atoms, respectively. Green spheres denote the edge C atoms stacking close to the fcc sites. (d) Atomic resolution CC-STM image of an α border ($V_b = -0.1$ V, $I_{\rm set} = 2$ nA). Blue mesh and red pattern are the Ir(111) and G cells sketched from the atomic structures of both regions, respectively. Gray arrows indicate the Ir-G border. Each moiré structural region in G is identified from the comparison of the C ring center positions with the stacking sites extracted from the atomic positions of the Ir(111) substrate. The green folded line is the connection of the outermost sites of the honeycomb cells towards the Ir region. The yellow zigzag line indicates the positions of missing C atoms under the assumption of an extension of the honeycomb lattice towards the Ir region.

force for the formation of straight and kinked step edges of G islands.

A careful inspection of the CC-STM images of the *borderlike* edge shows that the moiré-periodic modulation has two variants. The STM image of Fig. 3(a) shows two *borderlike* edges oriented with a relative angle of 120°. The mesh indicates the moiré lattice with ONT regions located at the crossing points. For the upper part of the image, the protruding kinks of the G edge towards the Ir terrace are observed at the ONT regions. For the lower part, the protruding kinks are observed along the edge between the ONT regions. We call the former α border, and the later β border, respectively.

To interpret the difference between the atomic stacking of α and β border, let us consider first the two types of Ir(111) step edges. A fcc(111) surface shows two different types of monatomic step edges, depending on the positions of the nearest atoms in the lower terrace. One discriminates so called A and B facets.[19] An alternation between the two types of monatomic steps exists along a step edge on a fcc(111) surface, when an angle of 120° separates two segments of the edge. The step edge of the Ir terrace shown in Fig. 3(a) is an example of such a situation where both A- and B-type monatomic steps exist. To facilitate the discussion we present in Figs. 3(b) and 3(c) a hard sphere model of the unrelaxed atomic positions of the G sheet in the proximity to the A- and B-step edges of Ir(111), respectively. In these figures the green spheres denote the edge C atoms stacked closest to a fcc site on top of the Ir lattice. In the case of the A step, the fcc sites of the lower terrace closest to the step edge are located in the ONT region. However, in the case of the B step, the fcc sites closest to the step edge are located between the ONT regions.

Figure 3(d) is an atomic resolution CC-STM image of an α border. The bright contrast on the left side corresponds to the atomic positions of Ir. On the right side it corresponds to the bond between C atoms along the sides of a honeycomb cell of G. We determine the stacking types and the structural environment of G from a careful inspection of the location of the bright contrast of the honeycomb structures in the image. The G lattice comes into contact with the Ir terrace at the ONT region. In contrast, missing-atom positions (yellow zigzag line) are observed between ONT regions, as we observe in Fig. 3(d). On the left part of Fig. 3(d), a blue mesh follows the position of the centers of the Ir atoms on the top terrace. The extension of this mesh on the territory of the lower terrace corresponds to the fcc sites of the lower terrace. Interestingly, the positions of the outermost C atoms, as denoted by green dots, match the fcc sites of the Ir(111) surface. From these observations we identify the α border of Fig. 3(a) as being connected to the A step of Ir(111). As the counterpart, a β border corresponds to the B step of Ir(111). In both cases, it appears that G tends to protrude toward Ir where the stacking of the outermost C atoms of G are close to a fcc site of Ir(111). At a *borderlike* edge, introduction of Ir step edges tends to promote only the fcc site of Ir(111) as the favorable stacking site of the G edge atoms, in contrast to those in a *steplike* edge where no apparent difference is observed between two sites.

We performed spatially resolved STS measurements near G edges. Figure 4 shows the dI/dV spectra measured on different positions along the transition from G towards Ir across (a) *steplike* and (b) *borderlike* edges. As the measurement

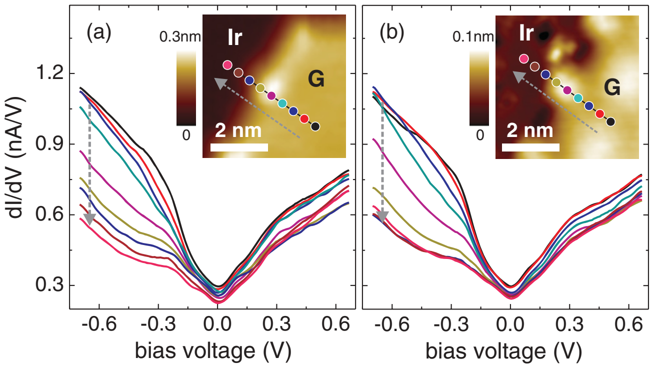

FIG. 4. (Color online) STS curves measured on different positions from G to Ir across (a) *steplike* and (b) *borderlike* edges ($V_{\rm stab} = 0.5$ V, $I_{\rm stab} = 1$ nA). The inset in each panel is the CC-STM image showing the positions where STS measurements were performed [$V_b = -0.05$ V, $I_{\rm set} = 1$ nA for (a) and $V_b = -0.2$ V, $I_{\rm set} = 1$ nA for (b)]. The color codes of the STS curves correspond to those of the positions in the inset for each panel.

positions move from G to Ir, the dI/dV signal decreases in magnitude for both types of edges. It approaches the values measured on Ir without the appearance of additional peaks. The variation of the dI/dV signal with position is more pronounced for negative V_b as compared to positive V_b. We find a monotonic variation of the dI/dV signal within the distance of ∼±1 nm from the edges, where peculiar edge-related states, which were discussed for other systems[9] or have been described in theory,[2] were not observed.

Recent ARPES studies for G on Ir(111)[11,12] reveal a negligible modification of the G π band by the G-substrate interaction in the energy range from ≈ -1 eV to E_F as compared to theory on free standing G.[1] However, Lacovig *et al.*[16] discuss, based on the *ab initio* calculations, that the interaction between a G edge and Ir is strong enough to induce a considerable reduction (∼50%) of the C-substrate distance near the edges as compared to that of central region of a G island on Ir(111). This structural relaxation should also impact the electronic DOS near an edge as compared to the central region of an island. The reduction of the dI/dV signal in Fig. 4, which can be attributed to the reduction of the G DOS at the edges, possibly reflects this.

A possibly strong edge-substrate interaction might arise from the broken σ orbitals of the G edge atoms. We speculate that an unsaturated σ orbital at the edge tends to bond to the Ir atoms with a covalent character, which would reduce the edge energy and deplete the DOS near E_F. This could explain the decrease of dI/dV signals in Figs. 4(a) and 4(b). Edge-substrate interaction in G/Ir(111) could also induce a considerable deviation of the orbital structures of the edge atoms from that of the sp^2 C-C bonding in the central region of G. Thus, electronic relaxation due to a C-Ir interaction could be the reason why our STS measurement do not show peculiar electronic states in the edge region, in contrast to the prediction of theory for the edge of free-standing G.[2]

In conclusion, we performed STM and STS on the edges of monolayer G on Ir(111). The atomic structure at the edge of a G island on Ir(111) depends strongly on the stacking configurations of the edge atoms, which are correlated with the moiré pattern of the G/Ir(111) system. The edges terminate with a zigzag carbon configuration and show periodic kinks in CC-STM images in the regions of the on-top stacked carbon rings. The periodicity is given by the moiré pattern of the G island. The termination of a G island at an Ir(111) step also leads to the formation of periodic kinks at the edge, where the kink position depends on the orientation of the Ir(111) step. Spatially resolved tunnel spectroscopy indicates a considerably reduced density of states near the edges of the G island. We tentatively ascribe these observations to the modified electronic bonding between edge C atoms and Ir lattice, where broken σ bonds of G, electronic relaxation, and G-Ir hybridization contribute. Future calculations are needed to clarify the connection between atomic structures and modified electronic DOS near the edges.

This work was partially supported by Deutsche Forschungsgemeinschaft Grant SFB 762. We thank N. Kurowsky for expert technical support.

---

[*] phark@mpi-halle.mpg.de

[1] A. H. Castro Neto, F. Guinea, N. M. R. Peres, K. S. Novoselov, and A. K. Geim, Rev. Mod. Phys. **81**, 109 (2009).

[2] K. Nakada, M. Fujita, G. Dresselhaus, and M. S. Dresselhaus, Phys. Rev. B **54**, 17954 (1996).

[3] S. Okada and A. Oshiyama, Phys. Rev. Lett. **87**, 146803 (2001).

[4] Y. Kobayashi, K. I. Fukui, T. Enoki, K. Kusakabe, and Y. Kaburagi, Phys. Rev. B **71**, 193406 (2005).

[5] Z. Klusek, W. Kozlowski, Z. Waqar, S. Datta, J. S. Burnell-Gray, I. V. Makarenko, N. R. Gall, E. V. Rutkow, A. Y. Tontegode, and A. N. Titkov, Appl. Surf. Sci. **252**, 1221 (2005).

[6] Y. Niimi, T. Matsui, H. Kambara, K. Tagami, M. Tsukada, and H. Fukuyama, Phys. Rev. B **73**, 085421 (2006).

[7] G. M. Rutter, N. P. Guisinger, J. N. Crain, P. N. First, and J. A. Stroscio, Phys. Rev. B **81**, 245408 (2010).

[8] K. A. Ritter and J. W. Lyding, Nat. Mater. **8**, 235 (2009).

[9] C. Tao, L. Jiao, O. V. Yazyev, Y.-Z. Chen, J. Feng, X. Zhang, R. B. Capaz, J. M. Tour, A. Zettl, S. G. Louie, H. Dai, and M. F. Crommie, Nat. Phys. **7**, 616 (2011).

[10] C. Busse, P. Lazić, R. Djemour, J. Coraux, T. Gerber, N. Atodiresei, V. Caciuc, R. Brako, A. T. N'Diaye, S. Blügel, J. Zegenhagen, and T. Michely, Phys. Rev. Lett. **107**, 036101 (2011).

[11] I. Pletikosić, M. Kralj, P. Pervan, R. Brako, J. Coraux, A. T. N'Diaye, C. Busse, and T. Michely, Phys. Rev. Lett. **102**, 056808 (2009).

[12] M. Kralj, I. Pletikosić, M. Petrović, P. Pervan, M. Milun, A. T. N'Diaye, C. Busse, T. Michely, J. Fujii, and I. Vobornik, Phys. Rev. B **84**, 075427 (2011).

[13] A. T. N'Diaye, J. Coraux, T. N. Plasa, C. Busse, and T. Michely, New J. Phys. **10**, 043033 (2008).

[14] J. Coraux, A. T. N'Diaye, M. Engler, C. Busse, D. Wall, N. Buckanie, F.-J. M. zu Heringdorf, R. van Gastel, B. Poelsema, and T. Michely, New J. Phys. **11**, 039801 (2009).

[15] S. K. Hämäläinen, Z. Sun, M. P. Boneschanscher, A. Uppstu, M. Ijäs, A. Harju, D. Vanmaekelbergh, and P. Liljeroth, Phys. Rev. Lett. **107**, 236803 (2011).

[16] P. Lacovig, M. Pozzo, D. Alfé, P. Vilmercati, A. Baraldi, and S. Lizzit, Phys. Rev. Lett. **103**, 166101 (2009).

[17] S. Phark, J. Borme, A. León Vanegas, M. Corbetta, D. Sander, and J. Kirschner, ACS Nano **5**, 8162 (2011).

[18] D. Subramaniam, F. Libisch, Y. Li, C. Pauly, V. Geringer, R. Reiter, T. Mashoff, M. Liebmann, J. Burgdörfer, C. Busse, T. Michely, R. Mazzarello, M. Pratzer, and M. Morgenstern, Phys. Rev. Lett. **108**, 046801 (2012).

[19] R. Stumpf and M. Scheffler, Phys. Rev. Lett. **72**, 254 (1994); A step: ⟨110⟩/{100}, B step: ⟨110⟩/{111}.